

Interferometric Bloch-Siegert B₁⁺ mapping at 7T

Patrik Wyss¹, Shaihan J Malik², Vincent O Boer³, Johanna J Bluemink³, Alexander Raaijmakers³, Mustafa Cavusoglu¹, Peter Luijten³, Johannes J Hoogduin³, Giel Mens⁴, and Anke Henning^{1,5}

¹Institute for Biomedical Engineering, UZH and ETH Zurich, Zurich, Switzerland, ²Imaging Sciences and Biomedical Engineering, Kings College London, London, United Kingdom, ³University Medical Center Utrecht, Utrecht, Netherlands, ⁴Philips Healthcare, Best, Netherlands, ⁵Max Planck Institute for Biological Cybernetics, Tübingen, Germany

Introduction

Inhomogeneity of transmit radio-frequency (RF) fields (B₁⁺) at high static B₀ field strength can be addressed by RF shimming or multi-channel transmit RF pulse design using transmit array coils with 2 or more transmit channels. Both approaches rely on accurate determination of B₁⁺ fields produced by single coil elements within meaningful scan times. The large dynamic range of B₁⁺ fields from single coil elements challenges the accuracy of state-of-the-art B₁⁺ mapping techniques. To overcome this problem two distinct solutions have been suggested recently: (1) Bloch-Siegert effect based B₁⁺ mapping [1] offers a large dynamic range and (2) B₁⁺ mapping using linear combinations of transmit channels enables accurate prediction of single channel B₁⁺ fields with increased signal-to-noise even if the underlying B₁⁺ mapping method has a small dynamic range [2-4]. **In this work**, both approaches are combined and hence interferometric Bloch-Siegert (BS) B₁⁺ mapping is introduced. The method was cross-validated against interferometric B₁⁺ mapping based on actual flip angle imaging (AFI) [2-3] as well as single channel transmit AFI B₁⁺ mapping.

Materials and Methods

Measurements were performed on a 7T whole body MRI system (Philips Healthcare, Best, Netherlands and Cleveland, USA) equipped with eight 1 kW transmit channels and an 8-channel transmit head coil (RAPID Biomedical) with a 16-channel receive array insert (NOVA Medical). Next to phantom measurements in two distinct phantoms: (A) a cylindrical sugar and salt water phantom mimicking the dielectric properties of brain tissue and (B) a spherical sunflower oil and tissue dielectric liquid phantom, two healthy volunteers were involved into the study after informed consent in line with local ethics regulations. A worst case SAR model limited the average forward power to a maximum of 8 W for the in vivo scans and to 15 W for the phantom study. Relative SAR values were double as high for BS (35% of the maximum allowed) in comparison to AFI (17%). Imaging parameters identical for all B₁⁺ mapping sequences were as follows: 2D; FOV 200 mm; in-plane resolution 3.2 mm; through-plane resolution: 4 mm, flip angle 60°, scan time per channel 62 s. RF pulses were scaled to an assumed B₁⁺ of 4μT in case of single channel transmission; 10μT in the case of interferometric phantom measurements and 16μT in case of all channel CP mode and interferometric in vivo measurements. The Bloch-Siegert (BS) implementation is gradient echo based and uses a Fermi RF pulse to induce the Bloch-Siegert effect, which was alternatively applied with positive or negative frequency offset to minimize sensitivity to B₀ inhomogeneities [1]. The following acquisition parameters have been used: BS pulse duration: 5ms; pulse offset: 6kHz; spoiling: 1ms, TE = 11ms, pulse area: 32.68 μT/ms, TR = 920ms / 1600ms (phantom / in vivo). The actual flip angle imaging (AFI) method was implemented according to Yarnykh et al [5] using a numerically optimized sinc-gauss RF excitation pulse with improved spoiling [6] and slice profile correction [7] with the following sequence parameters: TR 40 / 200 for phantom and 100 / 500 for in vivo measurements; TE 0.97 / 1.71 ms, NSA 4. For the interferometric B₁⁺ measurements the transmit phase was inverted consecutively for all 8 transmit channels according to [3-4]. Processing of the B₁⁺ maps was performed with custom written MATLAB code.

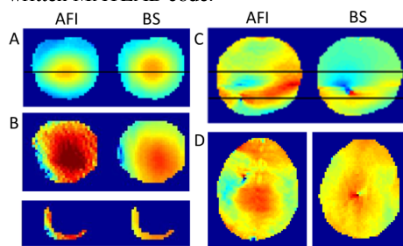


Figure 1: B₁⁺ maps acquired with actual flip angle imaging (AFI) versus Bloch-Siegert (BS) B₁⁺ mapping from a tissue dielectric phantom (A, B); an oil and tissue dielectric solution phantom (C) and the human brain (D) after phase shimming acquired with all eight channels (A,C,D) or with four channels using a 90° pre-pulse to create a black band feature (B, bottom).

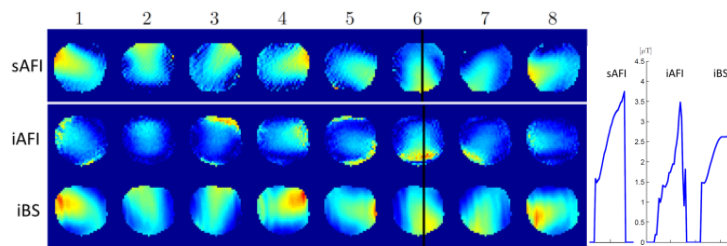


Figure 2: Single Channel B₁⁺ maps from a tissue dielectric phantom acquired by AFI with single channel transmission (sAFI); interferometric AFI (iAFI) and interferometric BS (iBS) and respective line plots for channels 6 along the black line.

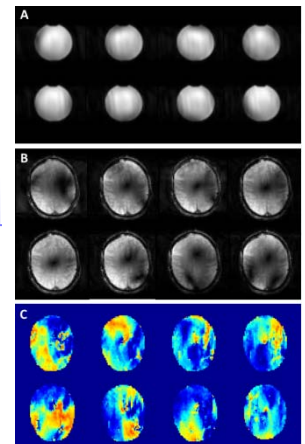


Figure 3: Interferometric BS single channel B₁⁺ mapping: the consecutive inversion of single channel transmit phases (A,B) leads to destructive interference resulting in signal dropouts in vivo (B), but not in the phantom experiments (A) shown in Fig 2. This negatively impacts the resulting quality of the derived in vivo single channel B₁⁺ maps (C).

Results and Discussion

General Validation: AFI and BS based B₁⁺ mapping reflect highly similar B₁⁺ pattern in different phantoms and the human brain (Figure 1), but only the BS method shows good SNR and accurate results across a wide range of transmit B₁⁺ field strength (1A, B). Both AFI and BS are robust in presence of inhomogeneous B₀ fields and chemical shift differences in the oil-tissue dielectric solution phantom, which is important for body applications. However, BS B₁⁺ mapping shows more realistic B₁⁺ field distributions with homogeneous B₁⁺ field in the oil and inhomogeneous but higher B₁⁺ field in the water fraction (1C) compared to AFI. Slice profile correction was necessary to prevent underestimation of the B₁⁺ field of 10-30% in 2D AFI, which is not necessary for the BS method since it relies on phase shifts instead of amplitude modulations. The BS method performed better in an accuracy test that aimed at predicting the position of a dark band produced by a saturation pre-pulse (nominal B₁⁺ 8 μT): BS 7.93±0.65μT versus AFI 7.97±2.06μT (Figure 1B, bottom).

Interferometric single channel B₁⁺ mapping: The combination of the interferometric approach with the Bloch-Siegert B₁⁺ mapping principle resulted in the largest dynamic range and best signal-to-noise ratio for determination of single channel B₁⁺ fields among all investigated methods in a phantom with tissue dielectric solution (Figure 2). The line plots in Figure 2 indicate that dynamic range problems of AFI might persist also in the interferometric approach and a single channel transmit strategy with prior adjustment of the pulse scaling towards the true average B₁⁺ might be the better strategy for AFI (Figure 2, sAFI). Due to duty cycle problems in case of long pulse durations at low B₁⁺ as produced by single channel transmission this approach is just feasible for AFI as a single pulse method. In contrast interferometric methods result in higher average B₁⁺ field strength and thus in shorter pulse durations and are hence hardware wise more applicable to B₁⁺ mapping methods with multiple pulses such as BS B₁⁺ mapping. In line with earlier observations by Malik [3] the numerical stability of interferometric B₁⁺ mapping depends on the dielectric properties and dimensions of the object as well as on the dynamic range of the B₁⁺ mapping method and needs to be optimized to the problem of interest, which might have influenced the iAFI results in Figure 2. In addition interferometric measurements based on phase inversion cause destructive interference, which can lead to local signal dropouts (Figure 3). While numerically less favorable interferometric encoding based on power scaling differences can avoid this problem.

In conclusion, interferometric Bloch-Siegert B₁⁺ mapping was introduced and shown to be superior in comparison to single channel transmit and interferometric AFI for single channel B₁⁺ mapping. However, interferometric B₁⁺ mapping approaches require careful optimization of the encoding scheme to avoid numerical instability and signal dropouts depending on the dynamic range of the B₁⁺ mapping method, the dielectric properties and dimensions of the object along with the initial shim set.

[1] Sacolick LI; Magn Reson Med. 2010;63:1315-1322.
[5] Yarnykh VL; Magn Reson Med. 2007;57:192-200.

[2] Nehrke K; Magn Reson Med. 2010;63:754-764.
[6] Nehrke K; Magn Reson Med 2009; 61:84-92.

[3] Malik SJ; Magn Reson Med. 2009; 62:902-909.
[7] Malik SJ; Magn Reson Med. 2011;65:1393-9.

[4] Brunner DO; Magn Reson Med. 2009; 61:1480-1488.